Postprint of: Hejna A., Barczewski M., Skórczewska K., Szulc J., Chmielnicki B., Korol J., Formela K., Sustainable upcycling of brewers' spent grain by thermo-mechanical treatment in twin-screw extruder, Journal of Cleaner Production (2020), 124839, DOI: 10.1016/j.jclepro.2020.124839

Sustainable upcycling of brewers` spent grain by thermo-mechanical treatment in twin-screw extruder

Aleksander Hejna[a,*], Mateusz Barczewski[b], Katarzyna Skórczewska[c], Joanna Szulc[d], Błażej Chmielnicki[e], Jerzy Korol[f], Krzysztof Formela[a,*]

[a]Department of Polymer Technology, Gdańsk University of Technology, Narutowicza 11/12 80-233 Gdańsk, Poland

[b]Institute of Materials Technology, Poznan University of Technology, Piotrowo 3, 61-138 Poznań, Poland

[c]Department of Polymer Technology, University of Science and Technology in Bydgoszcz, Seminaryjna 3, 85-326 Bydgoszcz, Poland

[f]Department of Food Industry Technology and Engineering, University of Science and Technology in Bydgoszcz, Seminaryjna 3, 85-326 Bydgoszcz, Poland

[e]Paint & Plastics Department in Gliwice, Institute for Engineering of Polymer Materials and Dyes, 50 A Chorzowska Street, 44 100 Gliwice, Poland

[f]Department of Material Engineering, Central Mining Institute, Pl. Gwarków 1, 40-166 Katowice, Poland

aleksander.hejna@pg.gda.pl, mateusz.barczewski@put.poznan.pl, katarzyna.skorczewska@utp.edu.pl, joanna.szulc@utp.edu.pl, b.chmielnicki@impib.pl, jkorol@gig.eu, kformela.ktp@gmail.com,

*Corresponding author's present address: Department of Polymer Technology, Chemical Faculty, G. Narutowicza Str. 11/12, Gdansk University of Technology, G. 80-233 Gdansk, Poland

Tel.: +48 58 347 2234; fax: +48 58 347 2134

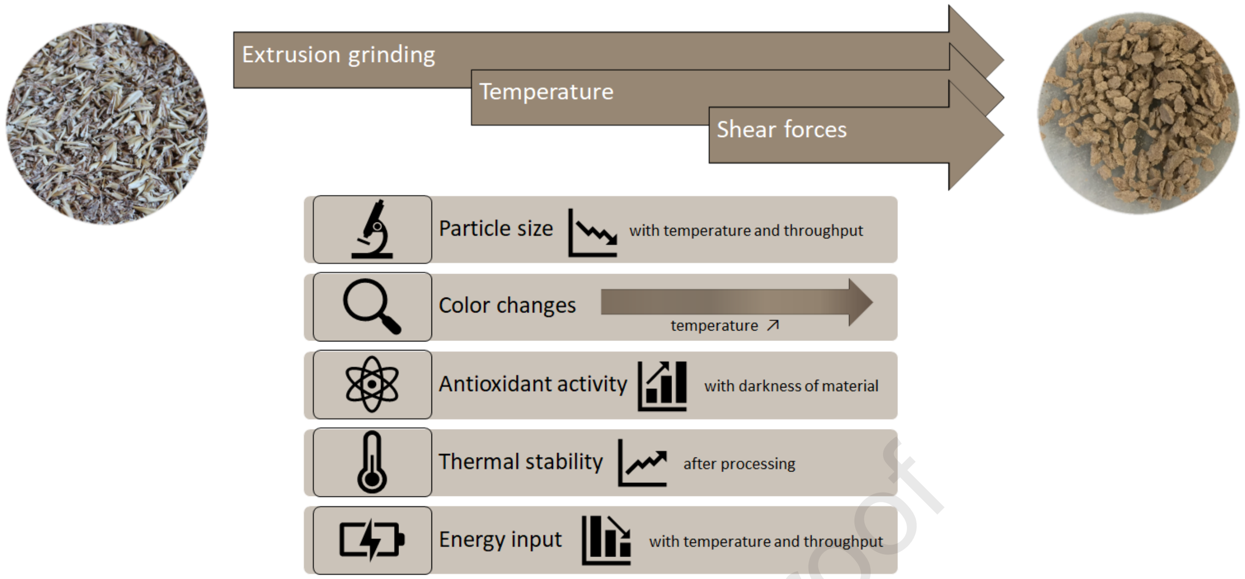
Extrusion grinding
Temperature
Shear forces
Particle size
with temperature and throughput
Color changes
temperature ↗
Antioxidant activity
with darkness of material
Thermal stability
after processing
Energy input
with temperature and throughput

Sustainable upcycling of brewers` spent grain by thermo-mechanical treatment in twin-screw extruder

Abstract

Thermo-mechanical treatment of brewers' spent grain (a by-product of beer manufacturing) was successfully performed via the extrusion process. The impact of temperature (from 30 to 180 °C), throughput (from 1 to 5 kg/h) and screw speed (from 75 to 375 rpm) on particle size, color, chemical structure, antioxidant activity and thermal stability of resulting material, as well as correlations between particular properties, were investigated. The color of treated brewers' spent grain was strongly influenced by particle size and the extent of Maillard reactions occurring during extrusion, responsible for the browning of material. Moreover, products of these reactions, melanoidins, enhanced the antioxidant activity of brewers' spent grain, which after extrusion at 180 °C was increased by even 100%. Thermo-mechanical treatment of brewers' spent grain at 120 and 180 °C increased its thermal stability investigated by thermogravimetric analysis. It was also observed that temperature treatment above 100 °C also led to the reduction in friction inside the extruder barrel and reduced by at least 20% specific mechanical energy required to brewers' spent grain modification, which positively affects the economic aspect of the process. The results confirm that a proper adjustment of extrusion parameters allows easy tailoring of the appearance (color, particle size distribution) and performance properties (thermal stability, antioxidant activity) of brewers' spent grain, which significantly extend applications of this cellulosic-rich waste in wood polymer composites technology.

Keywords

Brewers' spent grain; upcycling; thermo-mechanical treatment; extrusion; color and performance properties; chemical structure

1. Introduction

Wood polymer composites (WPCs) are a class of composites consisting of one or more lignocellulosic fillers and one or a mixture of polymeric materials. Thanks to the application of lignocellulosic fillers, these materials may be characterized, e.g., with lower density, higher stiffness, renewable nature, biodegradability, and reduced costs (Zajchowski and Ryszkowska, 2009). Moreover, due to lower hardness, the application of lignocellulosic filler reduces machine wear and damage of processing equipment comparing to, e.g., mineral fillers, commonly used in polymer composites.

In order to obtain WPCs with desired parameters, used fillers need to show particular properties. Fillers' properties affect the performance of the resulting WPCs. However, one of the most important is the particle size distribution. It was repeatedly proven that smaller particles often show higher specific surface areas, which together enhance the mechanical performance of composites (Fu et al., 2008). Moreover, the small particle size of filler may enhance the barrier properties of the composite, which can have an influence on, e.g., the rate of biodegradation (Kargarzadeh et al., 2017, 2018). Currently applied methods of size reduction of fillers are mostly based on processes with periodic character and use of various types of mills (Bridgeman et al., 2007; Silva et al., 2011). More perspective solutions, which are more cost-effective, should be based on continuous processes, such as extrusion, which was applied in the presented study.

Another parameter, essential for the applications of WPCs, affecting their aesthetic aspect is their color. Commonly used natural fillers may vary in color because of different type and source of raw material (e.g., different types of wood or other lignocellulosic fillers), but also because of the applied treatment, most often associated with size reduction. During grinding or milling of fillers, shear forces and sometimes also the temperature is applied to the material, which is inducing color changes of material.

Generally, changes in color during grinding of fillers are associated with two factors: final particle size and chemical reactions occurring inside the material during processing. The changes in the roughness of the surface, hence light scattering and particle size of fillers, significantly affect the light transmittance, which was confirmed for diverse natural materials (Bolade et al., 2009; Sun et al., 2016).

Chemical reactions resulting in the changes in color are generally referred to as non-enzymatic browning reactions. This group consists mainly of caramelization and Maillard reactions. The first reaction is a complex process of sugar pyrolysis, including, e.g., dehydration, condensation, fragmentation, isomerization, or polymerization reactions of sugars, resulting in the generation of caramelans ($C_{24}H_{36}O_{18}$), caramelens ($C_{36}H_{50}O_{25}$) and caramelins ($C_{125}H_{188}O_{80}$) (Villamiel et al., 2006). During caramelization, volatile compounds are also formed, which are responsible for characteristic caramel flavor. Maillard reactions, which involve chemical reactions between amino groups of amino acids and carbonyl groups of sugars, can take place at lower temperatures than caramelization. They involve reactions of reducing sugars with amino acids and result in the hard to characterize complex mixture of compounds responsible for the final color and flavor of resulting material, which is very important in polysaccharide-based food products, such as cookies, biscuits, bread, etc. (Maillard, 1912). Generally, a group of resulting products, responsible for the color change, is referred to as melanoidins – higher molecular weight oligomeric and polymeric substances (Martins et al., 2000). The general scheme of Maillard reactions, which show their complexity, is presented in Fig. S1. It is also crucial that melanoidins are commonly known in food chemistry and technology for their antioxidant activity, which enhances the storage stability of various food products (Pastoriza and Rufián-Henares, 2014; Rivero-Pérez et al., 2002). Therefore, based on the literature data, it can be assumed that they could also enhance the stability of WPCs (Moraczewski et al., 2019).

From an economical and ecological point of view, the most beneficial is the incorporation of fillers, which are considered as by-products or wastes resulting from the processing of renewable raw materials. Therefore, it seems very interesting for the manufacturing of polymer biocomposites to use the brewers' spent grain (BSG), which is the major by-product of the brewing industry, generated in the mashing process (Hejna et al., 2015). BSG shows relatively similar composition to various waste fillers applied during the preparation of WPCs, e.g., pulp resulting from the paper industry or wood flour. However, it contains significantly higher amounts of proteins, which can participate in Maillard reactions, enhancing the antioxidant activity of filler (Rufián-Henares and Morales, 2007). BSG stands for ~85% of the total by-products of beer manufacturing, and according to literature data, accounts for around 31% of the initial malt weight (Mussatto et al., 2006). According to The Brewers of Europe Beer Statistics Report from 2018 (The Brewers of Europe, 2018), European producers manufacture over 41 billion liters of beer each year, which results in the generation of over 2.5 million tonnes of BSG. Market Research Store reports that global production of WPCs is increasingly growing, from almost 3.5 million tonnes in 2015 to over 4.3 million tonnes in 2017, and is expected to reach over 6.0 million tonnes in 2020 (Market Research Store, 2018). Therefore, research associated with the development of this group of materials is very perspective. Assuming with average filler share of 50 wt.% in WPCs, the current demand on lignocellulosic fillers is around 2.2 million tonnes annually, so it can be seen that utilization of BSG produced only in Poland could be a significant contribution to WPCs market.

The main limitation related to the application of BSG in polymer composites is related to two factors: relatively high humidity and large particle size of this cellulosic-rich waste. The dried form of BSG is present in the market. Therefore this research work is focused on solving the issues related to the particle size of BSG and the characteristics of ground BSG.

So far, BSG has not been very often investigated as a filler for WPCs. In previous works, BSG was successfully applied as filler into rigid polyurethane foams (Formela et al., 2017; Hejna et al., 2017), natural rubber (Zedler et al., 2018, 2020), and poly(ε-caprolactone) (Hejna et al., 2015). Obtained results indicated that proteins present in BSG acted as plasticizers and reduced the adhesion to polymer matrices. Therefore, suitable treatment of BSG prior application in WPCs should be investigated in order to understand how the changes in the chemical structure of BSG affect their impact on compatibility with polymer matrices. Authors investigating polymer/BSG composites (Berthet et al., 2015; Cunha et al., 2014; Revert et al., 2017) studied the microscopic structure, mechanical, and thermal properties of obtained WPCs, which indicated insufficient interfacial adhesion between matrix and filler. The only modification of filler was alkali treatment applied by Berthet et al. (2015). However, they were not able to prepare WPCs due to the aggregation of the fibers. Therefore, the effect of treatment could not be evaluated. Moreover, the impact of melanoidins, potentially enhancing the resistance of composites towards oxidation, has not been investigated yet.

In this paper, sustainable upcycling of brewers` spent grain by thermo-mechanical treatment in the twin-screw extruder was developed. The twin-screw extruder was selected due to: i) high mixing and shearing efficiency of processed material; ii) common application in the industry (more straightforward implementation of laboratory results at industrial scale), and iii) continuity of process (high throughput and good repeatability of results). Recently, extrusion techniques found application in the treatment of biomass and lignocellulosic wastes (Duque et al., 2017; Leonard et al., 2019; Offiah et al., 2018). However, there is a lack of published information about the application of this technique for utilization or up-cycling of brewers` spent grain. Therefore, in this research work, the impact of extrusion conditions (temperature, throughput, screw speed) on the specific mechanical energy required to BSG particles size reduction, particle size distribution, chemical structure, color properties, thermal stability and antioxidant activity of treated BSG were investigated in order to evaluate the possibility of its application in wood polymer composites technology.

2. Experimental

2.1. Materials

Brewers' spent grain used in the presented study was obtained from Energetyka Złoczew sp. z o.o. (Poland). It was waste from the production of light lager and consisted solely of barley malts. The supplier already dried obtained BSG. In Fig. 1, there is shown the appearance of used BSG.

Synthetic 2,2-diphenyl-1-picrylhydrazyl (DPPH) radical (≥95%, solid crystal) and 70% water solution of ethanol were used during the determination of the antioxidant activity of modified BSG. Both compounds were acquired from Sigma Aldrich (Poland) and used as received.

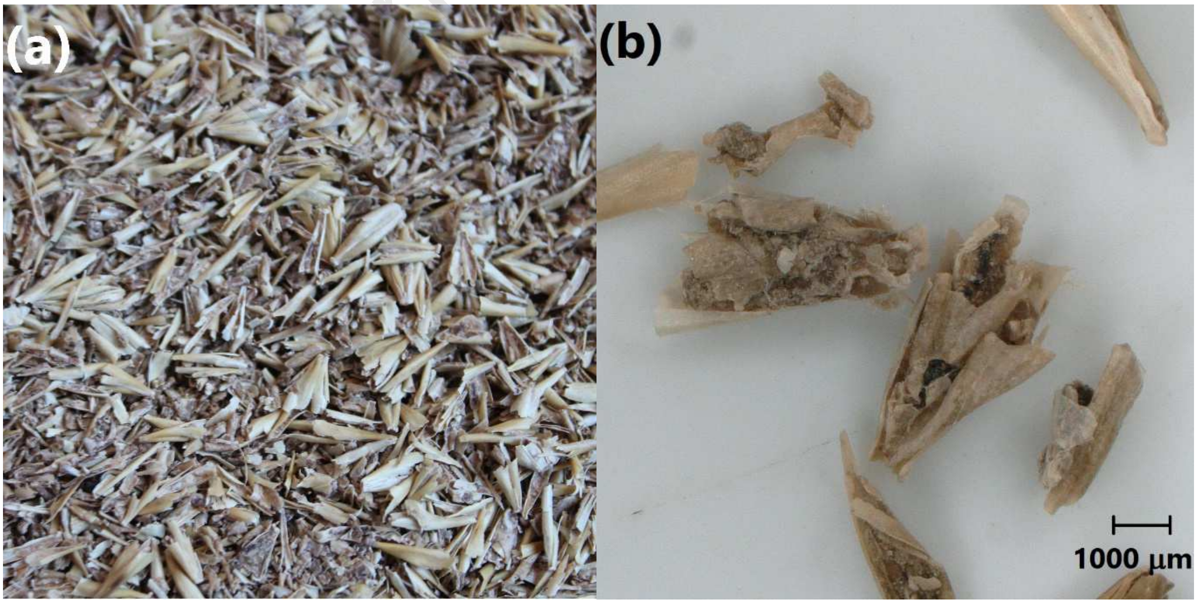

Figure 1. Macroscopic (a) and microscopic (b) appearance of applied BSG before extrusion grinding.

2.2. Extrusion grinding of BSG

Extrusion grinding of BSG was performed with EHP 2x20 Sline co-rotating twin-screw extruder from Zamak Mercator (Poland), following patent application (Hejna and Formela, 2019). The extruder has eleven heating/cooling zones with a screw diameter of 20 mm and an L/d ratio of 40. The screw configuration is shown in Fig. S2. BSG was dosed into the extruder by a volumetric feeder with a constant throughput of 1, 3, or 5 kg/h. Screw speed varied from 75 to 225, from 150 to 300 and from 225 to 375 rpm, respectively, for increasing throughput. Barrel temperature in all zones was set at 30, 60, 120, or 180 °C. For each set of parameters, extrusion was carried out for at least 60 minutes after stabilization of the motor load of the extruder, which indicated stabilization of the process. After grinding, samples of BSG were left in order to cool down to room temperature. Samples were coded as X/Y/Z, where X stands for the processing temperature, Y for the throughput, and Z for the screw speed.

2.3. Characterization techniques

The characterization of the particle size distribution of investigated BSG fillers was evaluated using a laser particle sizer Fritsch ANALYSETTE 22 apparatus operated in the range of 0.08 - 2000 µm.

The chemical structure of studied samples was determined using Fourier transform infrared spectroscopy (FTIR) analysis performed by a Nicolet Spectrometer IR200 from Thermo Scientific (USA). The device had an ATR attachment with a diamond crystal. Measurements were performed with 1 cm^{-1} resolution in the range from 4000 to 400 cm^{-1} and 64 scans. For each sample, at least three spectra were recorded.

The color of treated BSG was evaluated according to the Commission Internationale de l'Eclairage (CIE) through L*a*b* coordinates (International Commission on Illumination, 1978). In this system, L* is the color lightness (L*=0 for black and L*=100 for white), a* is the green(-) / red(+) axis, and b* is the blue(-) / yellow(+) axis. Thirty tests of each sample were done and used for the determination of arithmetic mean values. The color was determined by optical spectroscopy using HunterLab Miniscan MS/S-4000S spectrophotometer, placed additionally in a specially designed light trap chamber. The total color difference parameter (ΔE*) was calculated according to the following formulation (1) (Bociaga and Trzaskalska, 2016):

$$\Delta E^{*} = [(\Delta L^{*})^{2} + (\Delta a^{*})^{2} + (\Delta b^{*})^{2}]^{0.5} \quad (1)$$

Moreover, obtained values of a* and b* may be used to calculate other parameters used to describe colors, such as chroma and hue, defined by the following equations (2 and 3):

$$C_{ab}^{*} = (a^{*2} + b^{*2})^{\frac{1}{2}} \quad (2)$$

$$h_{ab} = tan^{-1}\left(\frac{b^{*}}{a^{*}}\right) \quad (3)$$

Determined color parameters were also converted to the commonly used Adobe RGB color space defined by the three chromaticities of the red, green, and blue additive primaries (Hunt, 2004). The first step was the conversion from CIELab to normalized CIEXYZ space according to the following equations (4-8) (Lopez et al., 2005):

$$X = X_{w} f^{-1}\left(\frac{L^{*}+16}{116} + \frac{a^{*}}{500}\right) \quad (4)$$

$$Y = Y_{w} f^{-1}\left(\frac{L^{*}+16}{116}\right) \quad (5)$$

$$Z = Z_{w} f^{-1}\left(\frac{L^{*}+16}{116} - \frac{b^{*}}{200}\right) \quad (6)$$

where:

$$f^{-1}(t) = \begin{cases} t^{3} & t > \delta \\ 3\delta^{2}\left(t - \frac{4}{29}\right) & otherwise \end{cases} \quad (7)$$

and

$$\delta = \frac{6}{29} \quad (8)$$

and

X_w, Y_w and Z_w are the values for the reference white point, which for Iluminant D65 equal 0.950450, 1.000000 and 1.088754, respectively, according to ITU-R Recommendation BT.709.

Next, conversion from CIEXYZ color space to linear RGB (υ) was made according to the following formulas (9-20):

$$\begin{bmatrix} r \\ g \\ b \end{bmatrix} = [M]^{-1} \begin{bmatrix} X \\ Y \\ Z \end{bmatrix} \quad (9)$$

where:

$$[M] = \begin{bmatrix} S_r X_r & S_g X_g & S_b X_b \\ S_r Y_r & S_g Y_g & S_b Y_b \\ S_r Z_r & S_g Z_g & S_b Z_b \end{bmatrix} \quad (10)$$

where:

$$X_r = \frac{x_r}{y_r} \quad (11)$$

$$Y_r = 1 \quad (12)$$

$$Z_r = \frac{(1 - x_r - y_r)}{y_r} \quad (13)$$

$$X_g = \frac{x_g}{y_g} \quad (14)$$

$$Y_g = 1 \quad (15)$$

$$Z_g = \frac{(1 - x_g - y_g)}{y_g} \quad (16)$$

$$X_b = \frac{x_b}{y_b} \quad (17)$$

$$Y_b = 1 \quad (18)$$

$$Z_b = \frac{(1-x_b-y_b)}{y_b} \quad (19)$$

$$\begin{bmatrix} S_r \\ S_g \\ S_b \end{bmatrix} = \begin{bmatrix} X_r & X_g & X_b \\ Y_r & Y_g & Y_b \\ Z_r & Z_g & Z_b \end{bmatrix}^{-1} \begin{bmatrix} X_w \\ Y_w \\ Z_w \end{bmatrix} \quad (20)$$

and:

(x_r, y_r), (x_g, y_g), and (x_b, y_b) are chromaticity coordinates of RGB system, which in the case of Adobe RGB are (0.64, 0.33), (0.21, 0.71) and (0.15, 0.06), while X_w, Y_w and Z_w are the values for the reference white point, as mentioned above (Adobe Systems Incorporated, 2005).

Conversion from linear RGB (υ) to nonlinear RGB (V) was made using gamma companding according to the following equation (21):

$$V = \upsilon^{\frac{1}{\gamma}} \quad (21)$$

where γ stands for gamma value characteristic for a color system, in the case of Adobe RGB equals 2.2.

Obtained RGB values were in the nominal range [0.0, 1.0]. In order to present them in the most commonly used range of [0, 255], components were multiplied by 255.

Samples of extruded BSG for the determination of antioxidant activity were prepared by the extraction of proper compounds in the following manner. Samples with a mass of 1 g were weighed on analytical balance with an accuracy of 0.001 g and then mixed with 9 cm^3 of 70% solution of ethanol. The mixtures were shaken vigorously and allowed to stand at room temperature in the dark for 20 hours. All extracts were centrifuged in a centrifuge Hettich Rotina 380 for 3 minutes at 3500 rpm. Subsequently, the antioxidant activity of supernatants was determined with a modified method described by Brand-Williams et al. (1995) using synthetic DPPH radical – 2,2-diphenyl-1-picrylhydrazyl. Three specimens were analyzed for each sample. For each analysis, 1 ml of analyzed extract was mixed with 5 ml of the 0.5 mM DPPH solution. The absorbance of the mixtures (A_i) was measured at 517 nm after 15 minutes of incubation at room temperature. The negative control (A_0) was prepared for 1 ml of 70% ethanol. The percent DPPH scavenging effect was calculated by using the following equation (22):

$$I_{\%} = \frac{(A_0 - A_i)}{A_0} \cdot 100\% \quad (22)$$

The thermal analysis was performed using the TG 209 F3 apparatus from Netzsch (Germany). Samples of composites weighing approx. 10 mg were placed in a ceramic dish. The study was conducted in an inert gas atmosphere - nitrogen in the range from 30 to 900 °C with a temperature increase rate of 10 °C/min. Two specimens were analyzed for each sample.

In order to evaluate the effect of barrel temperature on the progress of ground tire rubber reclamation, the specific mechanical energy (SME, in kWh/kg) was determined. SME was calculated using equation (23):

$$SME = \frac{N}{Q} \quad (23)$$

where N is the consumption of drive motor power (kW), and Q is throughput (kg/h). For calculations of the specific mechanical energy, the average motor load from at least 60 minutes of extrusion was used.

3. Results and discussion

3.1. Particle size distribution

Fig. 2 shows the particle size distribution of the selected filler samples in order to determine its dependence on the adjusted extrusion parameters. The impact of process temperature on the particle size of obtained samples (for throughput of 3 kg/h and a screw speed of 225 rpm) is presented in Fig. 2a-d. It can be seen that lower extrusion temperatures, below 100 °C, resulted in larger particle sizes, due to the agglomeration of treated BSG related to higher moisture content. At lower temperatures (30 and 60 °C), moisture present in the BSG due to its hygroscopic nature (as other lignocellulosic materials) combined with the external forces causes granulation of particles. Such an effect is related to the enhanced hydrogen bonding between lignocellulosic particles caused by the presence of moisture (Sahputra et al., 2019). As a result, particles bigger than 1200 μm were present in extruded material, which is presented in Fig. 2a and 2b. Such an effect is often observed during extrusion cooking and used in the manufacturing of grain flakes and snacks (Dhanalakshmi et al., 2011). The appearance of these particles is presented in Fig. S3. The increase of the process temperature to 120 °C resulted in the reduction of average particle size, which is related to the lower share of particles bigger than 300 μm, and lack of agglomerates. Nevertheless, only for the temperature of 180 °C distribution of particle, diameters were noticeably more homogenous, comparing to lower temperatures. Such an effect was probably associated with the lower moisture content and partial decomposition of the extractives and other low molecular weight components of BSG (Mahmood et al., 2013).

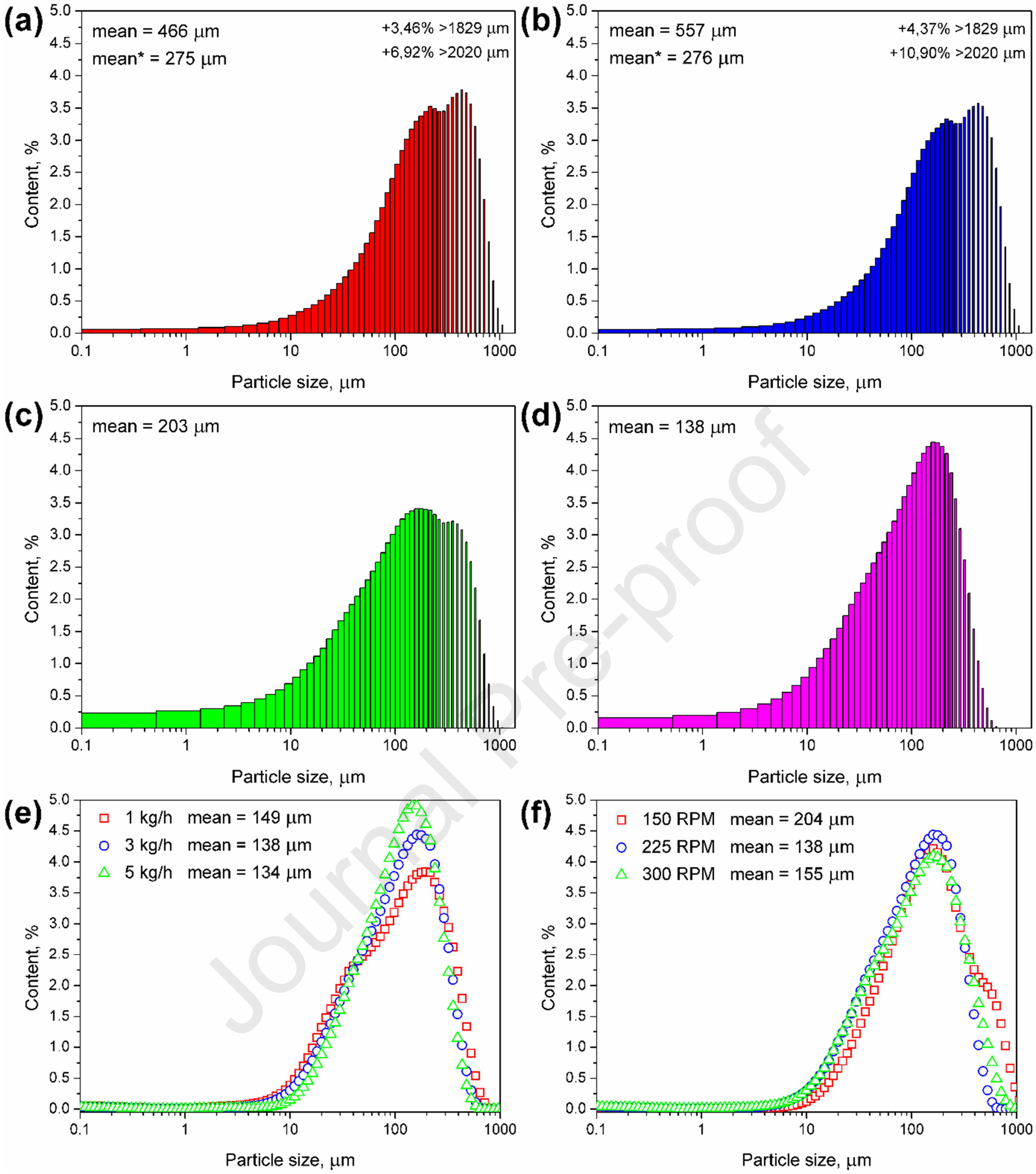

Figure 2. The particle size distribution of samples extruded with a screw speed of 225 rpm and throughput of 3 kg/h at (a) 30 °C, (b) 60 °C, (c) 120 °C and (d) 180 °C, as well as the impact of (e) throughput and (f) screw speed on particle size distribution.

Fig. 2e shown the impact of the extrusion throughput on the particle size distribution of ground BSG (for process temperature of 180 °C and a screw speed of 225 rpm). Throughput is associated with the degree of fill of extruder barrel, hence the level of shear forces between the BSG particles and between particles and extruder barrel (Kao and Allison, 1984). Suparno et al. (2010) developed a model based on experimental data, which indicates that shear forces are significantly increasing with the degree of fill of extruder barrel. However, an increase in throughput shows the opposite effect because it is associated with shorter residence time in the extruder and its more homogenous distribution (Altomare and Ghossi, 1986). In the presented case, it resulted in noticeably more homogenous particle size distribution and slightly smaller average particle size (Yeh et al., 1992). Such effect may be considered very beneficial from the potential application point of view (e.g., in wood polymer composites) because it enables the preparation of material showing superior properties with higher efficiency.

The plot in Fig. 2f presents the impact of screw speed on the particle size distribution of BSG ground at 180 °C and with a throughput of 3 kg/h. It can be seen that despite the similar distribution of particle size, differences between screw speed of 150 rpm and higher values were noted. Such an effect is associated with the increase of shear forces inside the extrusion barrel for higher screw speed values, which facilitate the disintegration of BSG particles. A similar effect was observed for the extrusion treatment of ground tire rubber particles by Formela et al. (2014). On the other hand, similar to throughput, an increase of screw speed shows opposite effects associated with the shortening of material’s residence time in the extruder barrel. As a result, the increase of screw speed over 225 rpm for analyzed process parameters increased average particle size.

3.2.Color properties

The color parameters of prepared BSG samples are presented in Table 1. As mentioned above, in section 2.3. Measurements, the color of materials was evaluated using CIELab color space, and then parameters were converted to popular Adobe RGB space. Moreover, the total color difference parameter (ΔE*) related to the unprocessed reference sample is presented, as well as the color of obtained materials.

Table 1. Color parameters of extruded BSG samples and antioxidant activity of selected samples.

Temperature, °C	Throughput, kg/h	Screw speed, rpm	Color parameters										Antioxidant activity towards DPPH, %
			L*	a*	b*	ΔE*	R	G	B	Color	C_{ab}*	h_{ab}, °	
Reference sample			48.17	5.11	13.04	-	124.8	110.3	93.8	🟫	14.0	68.6	36
30	1	75	49.87	4.66	12.14	1.97	128.3	114.6	99.1	🟫	13.0	69.0	-
		150	56.50	4.71	13.43	8.35	145.8	130.9	112.8	🟫	14.2	70.7	-
		225	56.81	4.88	13.91	8.69	147.0	131.6	112.8	🟫	14.7	70.7	-
	3	150	51.98	4.87	13.09	3.82	134.2	119.6	102.6	🟫	14.0	69.6	-
		225	50.97	4.61	12.31	2.94	131.1	117.3	101.4	🟫	13.1	69.5	49
		300	52.55	4.73	13.21	4.40	135.6	121.1	103.7	🟫	14.0	70.3	-
	5	225	50.37	4.80	12.45	2.30	129.8	115.8	99.8	🟫	13.3	68.9	-
		300	50.95	4.61	12.42	2.89	131.1	117.3	101.2	🟫	13.3	69.6	-
		375	53.44	5.03	13.70	5.32	138.3	123.1	105.1	🟫	14.6	69.8	-
60	1	75	50.64	4.44	12.23	2.68	130.0	116.6	100.7	🟫	13.0	70.0	-
		150	51.50	4.70	13.27	3.36	132.9	118.5	101.2	🟫	14.1	70.5	-
		225	52.89	4.65	13.50	4.76	136.5	122.0	104.1	🟫	14.3	71.0	-
	3	150	50.18	4.81	12.60	2.08	129.4	115.3	99.1	🟫	13.5	69.1	-
		225	49.60	4.60	11.83	1.94	127.4	114.0	98.9	🟫	12.7	68.8	49
		300	50.02	4.32	12.38	2.11	128.4	115.2	99.1	🟫	13.1	70.8	-
	5	225	50.41	4.69	12.59	2.32	129.9	115.9	99.7	🟫	13.4	69.6	-
		300	50.48	4.76	13.23	2.34	130.3	116.0	98.8	🟫	14.1	70.2	-
		375	51.35	4.84	12.67	3.21	132.4	118.1	101.7	🟫	13.6	69.1	-
120	1	75	57.64	5.32	14.52	9.59	149.9	133.4	113.8	🟫	15.5	69.9	-
		150	58.23	4.92	14.35	10.15	150.9	135.1	115.5	🟫	15.2	71.1	54
		225	56.55	5.15	14.33	8.48	146.8	130.7	111.5	🟫	15.2	70.2	-
	3	150	55.55	5.88	14.82	7.63	145.1	127.8	108.3	🟫	15.9	68.4	-
		225	56.29	5.42	14.14	8.20	146.3	129.9	111.2	🟫	15.1	69.0	54
		300	57.28	5.23	14.32	9.20	148.7	132.5	113.3	🟫	15.3	69.9	-

	5	225	57.15	5.50	14.46	9.10	148.7	132.0	112.8	🟫	15.5	69.2	-
		300	55.63	5.47	14.34	7.58	144.7	128.2	109.3	🟫	15.4	69.1	-
		375	56.32	5.42	14.29	8.25	146.4	130.0	111.0	🟫	15.3	69.2	-
180	1	75	45.26	7.91	15.18	4.57	121.1	101.7	84.0	🟫	17.1	62.5	-
		150	49.33	7.15	15.33	3.28	130.6	111.8	93.0	🟫	16.9	65.0	-
		225	50.30	6.82	15.34	3.57	132.8	114.3	95.2	🟫	16.8	66.0	63
	3	150	37.38	7.29	12.02	11.05	100.4	84.1	71.3	🟫	14.1	58.8	73
		225	47.23	7.68	15.23	3.50	125.8	106.4	88.3	🟫	17.1	63.2	71
		300	49.74	7.18	15.42	3.53	131.7	112.7	93.8	🟫	17.0	65.0	71
	5	225	42.43	7.57	13.59	6.27	113.3	95.3	80.0	🟫	15.6	60.9	-
		300	49.06	6.97	14.74	2.67	129.6	111.3	93.3	🟫	16.3	64.7	75
		375	48.46	7.31	15.28	3.15	128.6	109.6	91.1	🟫	16.9	64.4	-

As mentioned above, CIELab color space defines color with three parameters, L*, a*, and b*. According to equation (1), these parameters can be used to calculate the difference between the color of particular materials. According to standard ISO 2813:2001, the value of ΔE* is associated with the human ability to distinguish colors and notice the color difference (Bociaga and Trzaskalska, 2016).

Although all of them are affected by the physical structure of the material, the one most significantly affected by the particle size is lightness (Ahmed et al., 2014, 2015, 2016). Generally, independently of a* and b* parameters, hence hue of material, smaller particles show higher lightness, which is associated with the increase of specific surface area that allows more reflection of light (Chen et al., 1999; Horvath and Halasz-Fekete, 2005). In Table S1, there are summarized results published by other researchers, which confirm the presented results.

A similar phenomenon can be observed in the presented study. Most of the materials prepared at lower temperatures (30 and 60 ºC) had the highest values of average particle size among analyzed samples. As a result, they were characterized by similar color properties to the neat BSG. It was expressed by the values of ΔE* parameter lower than 3.5, which indicate invisible (ΔE* <1.0), small (ΔE* in the range of 1.0-2.0), or medium (ΔE* in the range of 2.0-3.5) color variations (Bociaga and Trzaskalska, 2016). Higher values, hence more significant color variations, were noted for samples extruded with higher screw speed, which reduced particle size and increased lightness of materials. Samples extruded at 120 °C show higher lightness comparing to lower extrusion temperatures, as a result of smaller particle size. Samples prepared at 180 °C were darker because of the chemical reactions occurring in the material and possible partial decomposition of polysaccharides present in BSG. Nevertheless, in Fig. 3, there is shown particle size distribution for the samples with the highest (120/1/150) and the lowest (180/3/150) lightness. It can be seen that except chemical reactions also particle size and its distribution shows a noticeable impact on the lightness of the material. Despite the better homogeneity of distribution for sample 180/3/150, the share of particles with lower diameters was higher for 120/1/150 samples. Hence its average particle size was lower. As a result, noticeable differences in lightness were observed, which, among other factors, was caused by different particle size distribution.

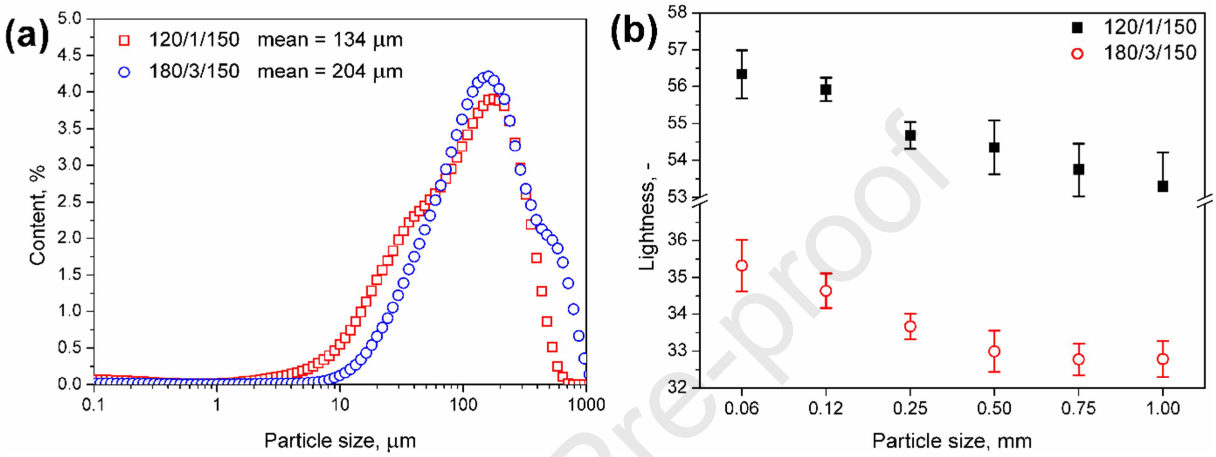

Figure 3. Particle size distribution for (a) samples with the lowest and the highest lightness and (b) fractions of these samples with various particle sizes.

For more detailed analysis, the samples mentioned above were fractionated using sieves with diameters of 0.06, 0.12, 0.25, 0.50, 0.75, and 1.00 mm, and their color parameters were determined. The obtained results are presented in Fig. 3b and confirm results published by other researchers (Kim and Shin, 2014; Liu, 2009).

As mentioned above, two groups of reactions are responsible for color changes in treated BSG: caramelization and Maillard reactions. In the presented case, caramelization does not play a significant role because it involves mono- and disaccharides, which are hardly present in brewers' spent grain (they are removed during mashing) and occurs at temperatures of 160 °C or higher, except fructose (110 °C) (Mussatto et al., 2006). Only minimal amounts of lower molecular weight saccharides may be generated during extrusion due to the shear-induced breakdown of glycosidic links (Ott, 1964). Therefore, for the investigated materials, caramelization reactions were not so significant, especially when processing temperatures of

30 and 60°C were applied. More critical are Maillard reactions, because they can take place at lower temperatures than caramelization. They involve reactions of reducing sugars, which can be present in BSG in the amount of ~15 wt.% (Waters et al., 2012). Except for typical reducing sugars, also other BSG compounds, lignin may show some reducing potential due to the presence of aldehyde groups, hence the ability to take part in Maillard reactions (Maillard, 1912). Moreover, BSG usually contains at least 15-20 wt.% of proteins, among which the most popular amino acids, which take part in Maillard reactions, are histidine, glutamic acid, lysine, and leucine (Lynch et al., 2016).

Products of Maillard reactions, e.g., melanoidins, are responsible for the change of BSG's color (Wang et al., 2011). One of the factors significantly affecting the final color change is reaction time, hence the residence time of material in the extruder. As proven by other researchers (Haugaard et al., 1951), the depth of color increases with the square of time. It is in line with the results of the presented study, which indicate that an increase of screw speed during treatment in extruder increased BSG's lightness (see Table 1). As mentioned above, also increasing throughput results in the shortening of residence time and exposition to elevated temperature (Yeh et al., 1992). Nevertheless, both screw speed and increased throughput may also show opposite effects, resulting in the enhancement of shear rate, hence shear forces acting on the material, which increases the temperature of the material and results in the darkening of material (Suprano et al., 2010). It can be seen that the increase in throughput caused a slight lowering of the lightness of BSG samples.

Except for lightness also other color properties, such as chroma or hue (presented in Table 1), are affected by the generation of melanoidins and resulting browning of BSG (Echavarria et al., 2013a). According to CIELab color space, typical brown color is characterized by a hue angle of ~50° (Berry, 1998). Therefore an increase of extrusion temperature enhances the browning of BSG related to the generation of melanoidins

(Maillard, 1912). Morales and van Boekel (1998) demonstrated a positive correlation between browning of casein/sugar solutions measured by spectrophotometer and chroma of generated melanoidins. Later, Wu et al. (2011) confirmed these findings for the malt drying process, during which chroma of malt was increasing with the content of melanoidins. Therefore, the observed increase of chroma value should be considered as a potential indicator of melanoidins' generation during extrusion grinding.

In the presented case, observed changes of color were not so strong because the absence of moisture during Maillard reactions tends to minimize browning, which can be noticed here, because of the relatively low moisture content of initial BSG (6.9 wt.%, according to TGA analysis). Nevertheless, the presented data indicate that the color of filler, which has a crucial impact on the appearance of the resulting composite (which is very important for the recipients of final products), depends on the processing conditions. In most cases, during the manufacturing of WPCs, filler pretreatment includes at least grinding aimed at achieving the desired particle size, which impacts the mechanical performance of the composite. Therefore, by adjustment of processing conditions, the desired color of the resulting filler can be achieved. As a result, it could significantly reduce or even eliminate the use of additional pigments or dyes, rarely composed only of natural compounds.

3.3.Antioxidant activity

For the manufacturing of WPCs, it can also be very interesting that melanoidins have been reported to show noticeable antioxidant activity. Hence, their presence, in combination with phenolic compounds (which can also be found in BSG), indicates that grinding may provide additional, antioxidant properties to BSG, simultaneously enhancing the durability of WPCs (Meneses et al., 2013). Such an effect was noted by other researchers for other natural fillers showing antioxidant activity (Sarasini et al., 2018). Iver et al. (2015) noted that the value of elongation at break was maintained at the same level after ten extrusion cycles for low-density polyethylene composites filled with 4, 8, and 12 wt.% of grape waste, turmeric waste and coffee grounds, respectively. Therefore, it is very interesting to investigate the antioxidant properties of thermo-mechanically treated BSG, which could potentially enhance the performance of WPCs. According to literature data, relatively high activity was observed for melanoidins based on histidine, which, as mentioned above, which is a significant amino acid of BSG (Yilmaz and Toledo, 2005). Based on these literature reports, further research was aimed to examine the antioxidant properties of selected samples of extruded BSG. The results of the performed tests are presented in Table 1.

Relatively high activity of the reference sample may be associated with the presence of phenolic compounds in BSG, such as ferulic and *p*-coumaric acids (Mussatto et al., 2006). It can be seen that performed modifications via extrusion grinding resulted in noticeable enhancement of BSG's antioxidant activity. The highest inhibition effect was noted for samples with the lowest lightness, which most likely contained the highest amount of melanoidins. It can also be seen that despite relatively similar values of lightness, BSG extruded at 120 and, especially at 180 °C showed higher antioxidant activity, suggesting a more intensive generation of melanoidins. The increase of samples' chroma may confirm such an assumption. A similar correlation between DPPH radical scavenging activity and a* and b*, hence also chroma values for melanoidins was observed by Echavarría et al. (2013b).

3.4.Fourier-transform infrared spectroscopy analysis

Fig. 4 shows the impact of the extrusion process and its parameters on the FTIR spectra of BSG. Generally, analyzed materials showed spectra typical for lignocellulose materials, such as wood flour, wheat bran, and others. All samples show typical signal (a) around 3290-3300 cm^{-1}, associated with the stretching vibrations of hydroxyl groups present in the structure of polysaccharides, as well as the NH stretching vibrations related to the presence of proteins in BSG (Mohsin et al., 2018). It can be seen that the intensity of this signal is hardly affected by the extrusion of material. Fig. 4b indicated that the most significant influence was noted for the screw speed, which directly affects the residence time and level of shear forces acting on the material. The increase of these forces results in the greater extent of materials decomposition and oxidation during the extrusion. In the range of 2850-2950 cm^{-1}, there are observed absorption bands (b) attributed to the symmetric and asymmetric stretching vibrations of C-H bonds in methyl and methylene groups. The extrusion treatment decreased the intensity of these bands, and it was more noticeable for BSG modified at higher temperatures. Such an effect is associated with a greater extent of polysaccharides decomposition and oxidation. Peaks (c) in the range of 1620-1700 cm^{-1} were related to the stretching vibrations of unconjugated C=O and C=C bonds in polysaccharides, but also to the amide I vibrations (stretching vibrations of C=O and C-N bonds in amide groups) (Barth, 2007). Their intensity was increased by the extrusion treatment, which points to oxidation of polysaccharides and the formation of melanoidins in Maillard reactions. Signals (d) in the range of 1515-1550 cm^{-1} are due to amide II vibrations – the combination of NH bending and CN stretching vibrations of amide groups. These signals, similar to (c), were affected by extrusion treatment. The changes in processing parameters strongly influenced the intensity of signals (c) and (d). Nevertheless, there was no straightforward impact because of the contradictory effects of screw speed and throughput, related to the strength of shear forces and residence time of material in the extruder barrel. Bands (e) and (f) in the range of 1220-1240 and 1030 cm^{-1} are associated with stretching vibrations of C-O and C=O bonds present in structures of polysaccharides (Hejna et al., 2020). The increase in their intensity confirms the oxidation of polysaccharides during grinding. Slight shifts of positions of signals associated with vibrations of carbon-oxygen are related to the chemical reactions occurring in the system and resulting in new interactions.

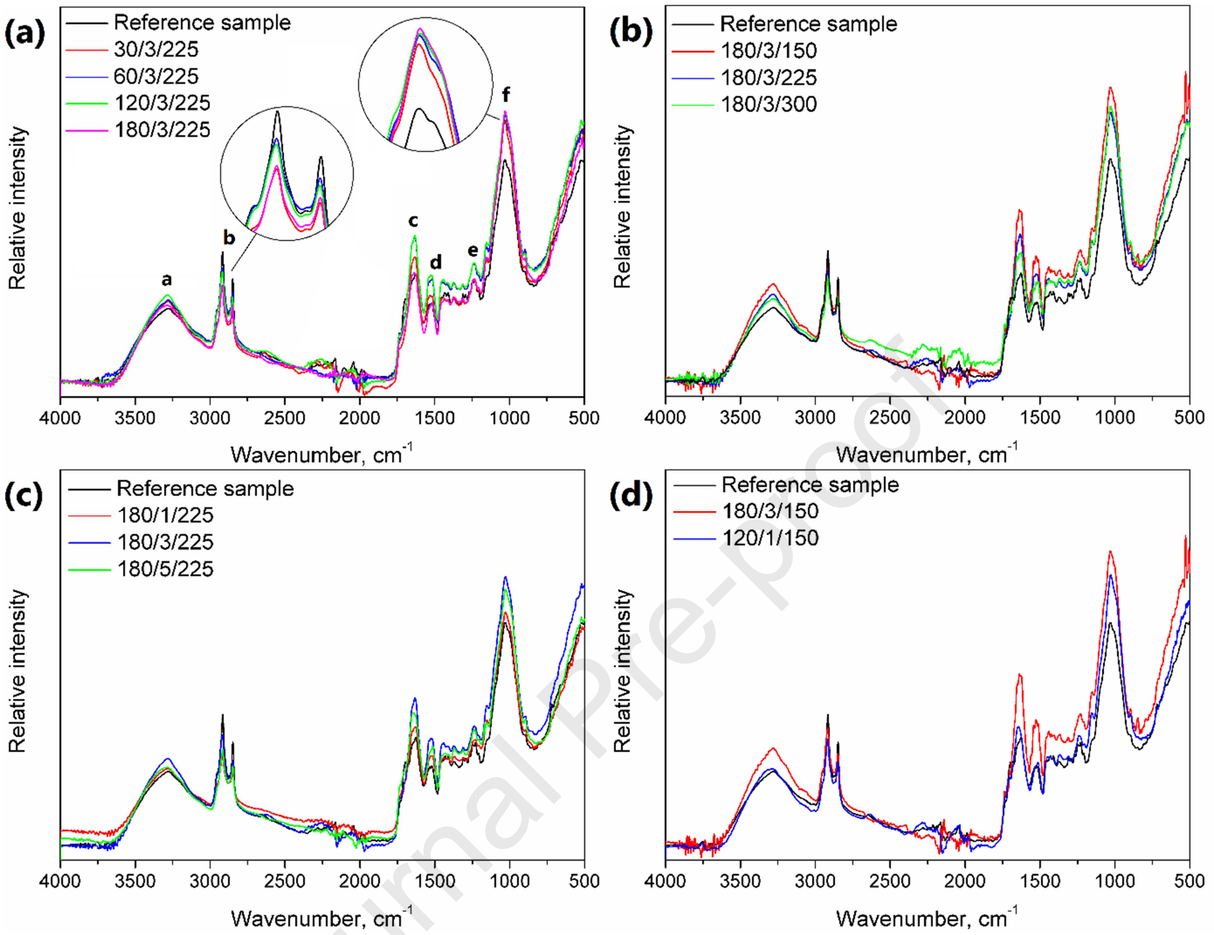

Figure 4. FTIR spectra of extruded BSG depending on (a) temperature, (b) screw speed, and (c) throughput of the process, as well as (d) spectra of samples with the lowest and the highest lightness.

Generally, presented FTIR spectra confirm the partial decomposition of polysaccharides during extrusion treatment followed by their oxidation and occurring Maillard reactions leading to the generation of melanoidins responsible for the color change. In Fig. 4b, the impact of screw speed on the FTIR spectra is presented. It can be seen that lower screw speed, hence longer residence time of material in the extruder, increased the intensity of signals associated with the reactions mentioned above occurring in the material. The most significant effect was noted for signal (f), which was related to the thermo-oxidation of material during treatment. FTIR spectra were also influenced by process throughput, hence the degree of fill, which affects the friction inside the barrel. Similar changes, compared to the reference material, were noted. However, the effect was weaker than for the screw speed, which suggests that residence time is a more significant factor than shear forces. Moreover, in Fig. 4d there are shown spectra for the lightest (120/1/150) and for the darkest sample (180/3/150), which indicates color changes were strictly associated with changes in the chemical composition of BSG.

3.5.Thermal stability

The results of the thermogravimetric analysis performed for samples of extruded BSG are presented in Fig. 5 and summarized in Table 2. It can be noticed that the extrusion process caused some changes in the thermal stability of the material. The reduction of moisture content was noted, which was measured as the magnitude of mass loss from 30 to 160 °C. It probably also included the decomposition of some extractives. However, it is here presented only for comparison purposes. The lowest content of moisture was noted for sample 180/3/225. It was mainly affected by the temperature of extrusion rather than throughput and screw speed, which, as mentioned before, show opposite effects associated with shear forces and residence time. The impact of extrusion temperature on the moisture content can be seen in Fig, 5a. In general, the presence of moisture in the modified BSG samples was associated with the hygroscopic character of natural fillers, which was confirmed by other researchers (Almeida et al., 2018; George et al., 2001). However, the reduction of moisture content was noted after treatment, which indicates changes in the polarity of the BSG surface. Nevertheless, even samples extruded at higher temperatures contained over 4.5 wt.% of moisture, which is still too much for the manufacturing of WPCs. Such values implicate the drying of filler before the manufacturing of composites, which is commonly applied practice.

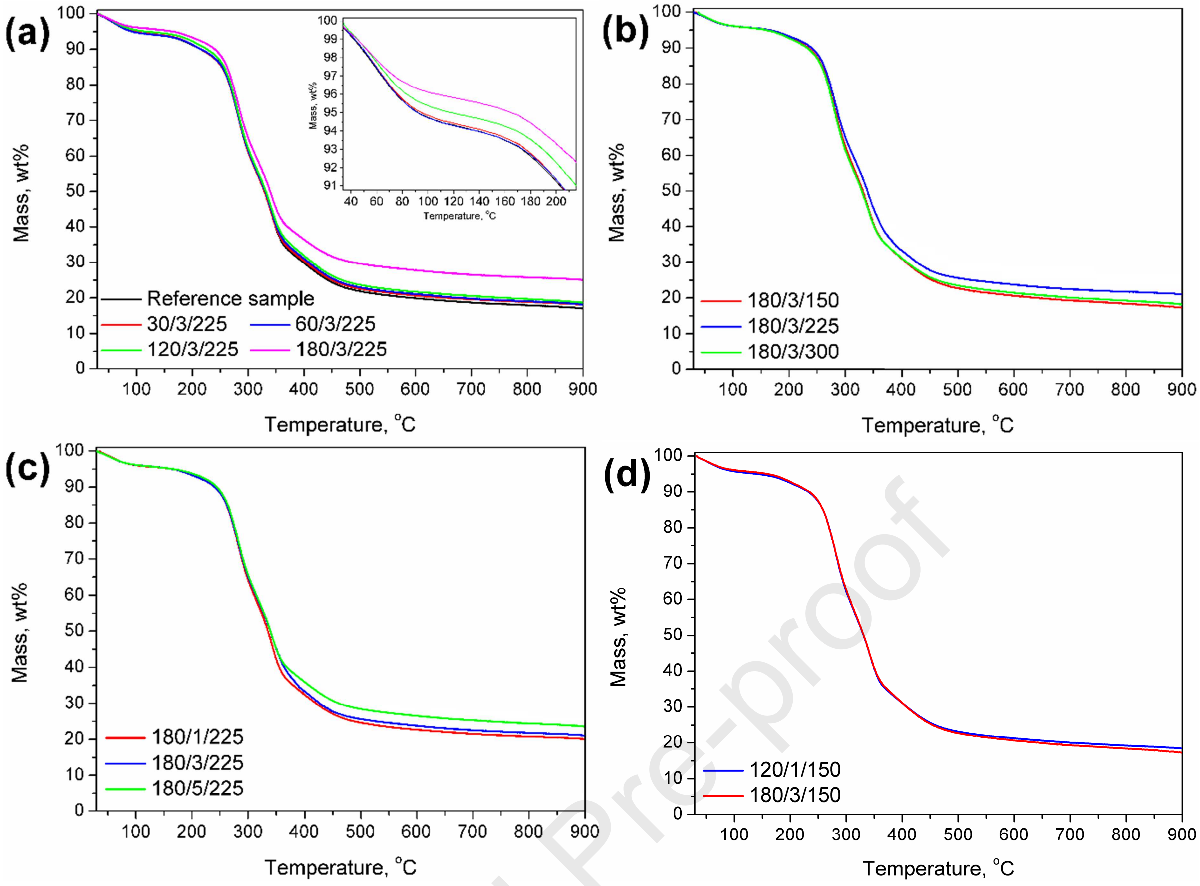

Figure 5. Thermogravimetric curves of extruded BSG depending on (a) temperature, (b) screw speed, and (c) throughput of the process, as well as (d) spectra of samples with the lowest and the highest lightness.

Generally, extrusion of BSG and increase of extrusion temperature enhanced BSG's thermal stability, which can be expressed by the rise of temperature associated with 5 wt.% mass loss during analysis ($T_{5\%}$). Such an effect can be associated with the reduction in the content of low molecular weight compounds, which may take part in Maillard reactions or can be degraded during processing at higher temperatures. Most of the weight loss of BSG occurs between 160 and 500 °C. In this range, there can be noticed two peaks on DTG curves, which are related to the decomposition of hemicelluloses and cellulose, ~281 and ~341 °C, respectively, which is in line with the results presented by other researchers (Vanreppelen et al., 2014). Independently of extrusion parameters, char yield at a temperature of 900 °C was very similar in the range of 18-19 wt.%, which is typical for BSG (Mahmood et al., 2013).

Table 2. Results of thermogravimetric analysis of extruded BSG samples.

Temperature, °C	Throughput, kg/h	Screw speed, rpm	Moisture content, wt.%	$T_{1\%}$, °C	$T_{5\%}$, °C	$T_{50\%}$, °C	T_{max1}, °C	T_{max2}, °C
Reference sample			6.90	43.7	91.7	332.6	281.1	346.8
30	3	225	6.05	43.0	95.4	329.1	281.2	341.4
60			6.20	42.8	92.3	329.9	281.3	342.0
120			5.50	44.6	117.1	332.1	280.7	342.3
180			4.65	45.1	159.3	340.0	282.0	340.2
180	3	150	4.70	45.5	162.9	332.4	279.5	341.3
		225	4.65	45.1	159.3	340.0	282.0	340.2
		300	4.85	46.8	152.7	332.3	281.0	342.0
180	1	225	4.85	46.1	157.2	335.0	281.4	344.1
	3		4.65	45.1	159.3	340.0	282.0	340.2
	5		4.65	45.2	162.2	340.0	281.2	341.8
120	1	150	5.10	44.7	139.2	332.3	280.7	342.7
180	3	150	4.70	45.5	162.9	332.4	279.5	341.3

3.6. Energy consumption

From the industrial point of view, an essential aspect of all processes included in the production cycle is energy consumption, which has a direct impact on the cost-efficiency of production. Grinding processes are considered as very energy-intensive. Therefore their investigations and optimization are significant (Li et al., 2012). On the other hand, twin-screw extrusion is considered a mechanical treatment method characterized by low energy demand (Rol et al., 2017). In Table 3, there are presented values of SME calculated according to equation (20) presented in 2.3. Measurements section. It can be seen that the amount of energy required to process BSG generally decreases with higher screw speed, which is directly associated with the residence time of material in the extruder barrel (Kelly et al., 2006). For higher temperatures, this effect was not so evident and strong, due to the above mentioned opposite effects of screw speed.

Table 3. Values of specific mechanical energy required for extrusion grinding of BSG under various conditions.

Temperature, °C	Throughput, kg/h	Screw speed, rpm	Motor load, %	SME, kWh/kg
30	1	75	55.5	0.872
		150	21.0	0.660
		225	13.5	0.636
	3	150	72.0	0.754
		225	41.5	0.652
		300	27.0	0.565
	5	225	76.5	0.721
		300	52.5	0.662
		375	37.0	0.581
60	1	75	42.0	0.660
		150	18.0	0.565
		225	11.5	0.542
	3	150	59.5	0.623
		225	35.0	0.550
		300	24.0	0.503
	5	225	64.0	0.603
		300	45.0	0.565
		375	34.5	0.542
120	1	75	23.5	0.369
		150	11.5	0.361
		225	8.5	0.400
	3	150	36.5	0.382
		225	19.5	0.306
		300	14.5	0.304
	5	225	34.5	0.325
		300	23.5	0.295
		375	19.5	0.306
180	1	75	26.0	0.408
		150	12.0	0.377
		225	8.5	0.400
	3	150	38.0	0.398
		225	19.0	0.298
		300	14.0	0.293
	5	225	29.5	0.278
		300	20.5	0.258
		375	17.0	0.267

At 30 and 60 ºC, SME was slightly increasing with throughput, which was associated with an increase in friction between the extruder barrel and processed material (Rasid and

Wood, 2003). At higher temperatures, friction was probably reduced due to the presence of a slight amount of water generated during Maillard reactions. It cannot be neglected that for materials processed with higher temperature values, i.e., 120 and 180 °C, low molecular weight products migrating from organic particles as well as decomposition products provide to the reduction of internal friction, which results in lowered SME values during extrusion.

Table 4. Dependence of SME on various extrusion parameters.

Dependence of SME vs								
Screw speed (R)			Temperature (T)			Throughput (Y)		
T, °C	Y, kg/h	R^2	Y, kg/h	R, rpm	R^2	T, °C	R, rpm	R^2
30	1	0.825	1	75	0.788	30	225	0.865
30	3	0.998	1	150	0.828	60	225	0.847
30	5	0.992	1	225	0.848	120	225	0.569
60	1	0.890	3	150	0.830	180	225	0.869
60	3	0.985	3	225	0.876			
60	5	0.980	3	300	0.886			
120	1	0.566	5	225	0.919			
120	3	0.769	5	300	0.912			
120	5	0.392	5	375	0.916			
180	1	0.062						
180	3	0.786						
180	5	0.302						

Table 4 presents the values of correlation coefficients (R^2) for dependences of SME vs. screw speed, temperature, and throughput. It can be seen that the best correlation can be observed for the temperature dependence of SME, which is in line with data presented by other researchers (Abeykoon et al., 2009, 2014). Lower values of R^2, observed mainly for the dependence of SME vs. screw speed at higher temperatures, are associated with very similar values of SME (see Table 3).

4. Conclusions

The structure and properties of brewers' spent grain subjected to extrusion grinding were investigated in order to determine its potential for application as filler for wood polymer composites. BSG was extruded in various conditions to analyze the impact of process temperature, throughput, and screw speed, which affect the magnitude of shear forces acting on material and material residence time in the extruder barrel. The most significant influence was observed for temperature since both throughput and screw speed show opposite effects.

In the case of particle size, very important for the manufacturing of WPCs, the rise of temperature led to more than two-fold size reduction, from 466 and 557 μm for 30 and 60 °C to 203 and 138 μm, respectively for 120 and 180 °C. In the case of lower temperatures, unfavorable granulation of BSG was observed, which on the other side could be desired, i.e., in the food industry. The influence of screw speed, and especially throughput, was not so significant.

Together with changes in chemical structure, particle size noticeably affected the color of the resulting material, which is crucial for the end-products users. The highest values of lightness, exceeding 55, were noted for samples extruded at 120 °C, so this parameter was increased by almost 15% despite occurring browning reactions (whose intensity was moderate at this temperature). Further rise of temperature resulted in the intensification of Maillard browning reactions and significant changes in BSG’s color. These changes were confirmed by FTIR analysis and rising antioxidant activity of material, which was associated with the presence of melanoidins, generated during processing. After extrusion at 180 °C, antioxidant activity was even doubled compared to the reference sample and 35% higher than after processing at 120 °C.

Higher processing temperatures also resulted in the enhancement of the thermal stability of BSG samples, which was related to the reduction of moisture content and possible partial decomposition and evaporation of its products. This phenomenon also favorably affected the specific mechanical energy required for extrusion of BSG, by reduction of internal friction inside the extruder barrel. For the temperatures of 120 and 180 °C, SME was in the range of 0.25-0.41 kWh/kg, comparing to 0.50-0.66 for 60 °C, and 0.56-0.87 for 30 °C. Such an effect may noticeably affect the economic aspect of BSG extrusion.

Generally, it was proven that extrusion of BSG might be considered an effective method for the preparation of fillers for WPC manufacturing, whose properties may be engineered by proper adjustment of extrusion parameters. Nevertheless, to enhance the industrial potential of the investigated process, the following issues should be addressed:

- emissions of volatile organic compounds should be analyzed, both in qualitative and quantitative terms, to determine the safety of the process considering health aspects,
- total energy use, related not only to the specific mechanical energy needed for screws rotation but also to heating the extrusion barrel, should be determined for different parameters of the process so that the economic calculations could be made,
- for similar reasons, the amount of water used during extrusion should be calculated and included in the economic calculations,
- the influence of BSG melanoidins generated during treatment on the resistance of various polymer matrices towards oxidation should be evaluated,
- the possibility of incorporation of additional modifiers enhancing the compatibility of modified BSG with polymer matrices should be evaluated.

These issues should be investigated in further works related to the thermo-mechanical treatment of brewers’ spent grain via the extrusion process.

Moreover, the presented results indicate that except for the application in the manufacturing of polymer composites, modified brewers’ spent grain may also be applied, e.g., as a functional food ingredient. According to the characteristics of the mashing process (source of BSG) and literature data, BSG contains very significant amounts of dietary fiber, which is very beneficial from the nutritional point of view. The increase of melanoidins content resulting from the extrusion treatment significantly increases the antioxidant activity of BSG. Therefore, it could be used as a substitute for conventional flour, simultaneously reducing the caloric value of food products and enhancing their shelf life.

Acknowledgments

This work was supported by the National Science Centre (NCN, Poland) in the frame of SONATINA 2 project 2018/28/C/ST8/00187 - *Structure and properties of lignocellulosic fillers modified in situ during reactive extrusion*.

Conflict of interest

On behalf of all authors, the corresponding author states that there is no conflict of interest.

References

Abeykoon, C., Kelly, A.L., Brown, E.C., Vera-Sorroche, J., Coates, P.D., Harkin-Jones, E., Howell, K.B., Deng, J., Li, K., Price, M., 2014. Investigation of the process energy demand in polymer extrusion: A brief review and an experimental study. Appl. Energ. 136, 726–737. https://doi.org/10.1016/j.apenergy.2014.09.024

Abeykoon, C., McAfee, M., Thompson, S., Li, K., Kelly, A.L., Brown, E.C., 2009. Investigation of torque fluctuations in extrusion through monitoring of motor variables, in: Proceedings of 26th PPS annual Europe/Africa regional meeting, Larnaca, Cyprus, paper no: 22-O.

Adobe Systems Incorporated, 2005. Adobe RGB (1998) Color Image Encoding, Version 2005-05. https://www.adobe.com/digitalimag/pdfs/AdobeRGB1998.pdf (accessed 18 April 2019).

Ahmed, J., Al-Attar, H., Arfat, Y.A., 2016. Effect of particle size on compositional, functional, pasting and rheological properties of commercial water chestnut flour. Food Hydrocolloid. 52, 888–895. https://doi.org/10.1016/j.foodhyd.2015.08.028

Ahmed, J., Al-Foudari, M., Al-Salman, F., Almusallam, A.S., 2014. Effect of particle size and temperature on rheological, thermal, and structural properties of pumpkin flour dispersion. J. Food Eng. 124, 43–53. https://doi.org/10.1016/j.jfoodeng.2013.09.030

Ahmed, J., Al-Jassar, S., Thomas, L., 2015. A comparison in rheological, thermal, and structural properties between Indian Basmati and Egyptian Giza rice flour dispersions as influenced by particle size. Food Hydrocolloid. 48, 72–83. https://doi.org/10.1016/j.foodhyd.2015.02.012

Almeida, G., Remond, R., Perre, P., 2018. Hygroscopic behaviour of lignocellulosic materials: Dataset at oscillating relative humidity variations. J. Build. Eng. 19, 320-333. https://doi.org/10.1016/j.jobe.2018.05.005

Altomare, R.E., Ghossi, P.,1986. An analysis of residence time distribution patterns in a twin screw cooking extruder. Biotechnol. Progr. 2 (3), 157–163. https://doi.org/10.1002/btpr.5420020310

Barth, A., 2007. Infrared spectroscopy of proteins. BBA-Bioenergetics 1767 (9), 1073–1101. https://doi.org/10.1016/j.bbabio.2007.06.004

Berry, B.W., 1998. Cooked color in high pH beef patties as related to fat content and cooking from the frozen or thawed state. J. Food Sci. 63 (5), 797–800. https://doi.org/10.1111/j.1365-2621.1998.tb17903.x

Berthet, M.A., Angellier-Coussy, H., Machado, D., Hilliou, L., Staebler, A., Vicente, A., Gontard, N., 2015. Exploring the potentialities of using lignocellulosic fibres derived from three food by-products as constituents of biocomposites for food packaging. Ind. Crop. Prod. 69, 110–122. https://doi.org/10.1016/j.indcrop.2015.01.028

Bociaga, E., Trzaskalska, M., 2016. Influence of polymer processing parameters and coloring agents on gloss and color of acrylonitrile-butadiene-styrene terpolymer moldings. Polimery 61, 544–550. https://doi.org /10.14314/polimery.2016.544

Bolade, M.K., Adeyemi, I.A., Ogunsua, A.O., 2009. Influence of particle size fractions on the physicochemical properties of maize flour and textural characteristics of a maize-based nonfermented food gel. Int. J. Food Sci. Tech. 44 (3), 646–655. https://doi.org/10.1111/j.1365-2621.2008.01903.x

Brand-Williams, W., Cuvelier, M.E., Berset, C., 1995. Use of a free radical method to evaluate antioxidant activity. LWT-Food Sci. Technol. 28 (1), 25–30. https://doi.org/10.1016/S0023-6438(95)80008-5

Bridgeman, T.G., Darvell, L.I., Jones, J.M., Williams, P.T., Fahmi, R., Bridgwater, A.V., Barracloigh, T., Shield, I., Yates, N., Thain, S.C., Donnison, I.S., 2007. Influence of particle size on the analytical and chemical properties of two energy crops. Fuel 86 (1-2), 60–72. https://doi.org/10.1016/j.fuel.2006.06.022

Chen, Q., Koh, H.K., Park, J.B., 1999. Color evaluation of red pepper powder. T. ASAE 42 (3), 749–752.

Cunha, M., Berthet, M.A., Pereira, R., Covas, J.A., Vicente, A.A., Hilliou, L., 2014. Development of polyhydroxyalkanoate/beer spent grain fibers composites for film blowing applications. Polym. Compos. 36 (10), 1859–1865. https://doi.org/10.1002/pc.23093

Dhanalakshmi, K., Ghosal, S., Bhattacharya, S., 2011. Agglomeration of food powder and applications. Crit. Rev. Food Sci. 51 (5), 432–441. https://doi.org/10.1080/10408391003646270

Duque, A., Manzanares, P., Ballesteros, M., 2017. Extrusion as a pretreatment for lignocellulosic biomass: Fundamentals and applications. Renew. Energ. 114, 1427–1441. https://doi.org/10.1016/j.renene.2017.06.050

Echavarría, A., Pagán, J., Ibarz, A., 2013a. Kinetics of color development of melanoidins formed from fructose/amino acid model system. Food Sci. Technol. Int. 20 (2), 119–126. https://doi.org/10.1177/1082013213476071

Echavarria, A., Pagan, J., Ibarz, A., 2013b. Optimization of Maillard reaction products isolated from sugar-amino acid model system and their antioxidant activity. Afinidad 70, 86–92.

Formela, K., Cysewska, M., Haponiuk, J., 2014. The influence of screw configuration and screw speed of co-rotating twin screw extruder on the properties of products obtained by thermomechanical reclaiming of ground tire rubber. Polimery 59 (2), 170–177. https://doi.org/10.14314/polimery.2014.165

Formela, K., Hejna, A., Zedler, Ł., Przybysz, M., Ryl, J., Saeb, M.R., Piszczyk, Ł., 2017. Structural, thermal and physico-mechanical properties of polyurethane/brewers' spent grain composite foams modified with ground tire rubber. Ind. Crop. Prod. 108, 844–852. https://doi.org/10.1016/j.indcrop.2017.07.047

Fu, S.Y., Feng, X.Q., Lauke, B., Mai, Y.W., 2008. Effects of particle size, particle/matrix interface adhesion and particle loading on mechanical properties of particulate–polymer composites. Compos. Part B-Eng. 39 (6), 933–961. https://doi.org/10.1016/j.compositesb.2008.01.002

George, J., Sreekala, M.S., Thomas, S., 2001. A review on interface modification and characterization of natural fiber reinforced plastic composites. Polym. Eng. Sci. 41 (9), 1471–1485. https://doi.org/10.1002/pen.10846

Haugaard, G., Tumerman, L., Silvestri, H., 1951. A Study on the Reaction of Aldoses and Amino Acids. J. Am. Chem. Soc. 73, 4594–4600. https://doi.org/10.1021/ja01154a028

Hejna, A., Formela, K., 2019. Sposób suszenia i rozdrabniania młóta browarnianego. Polish patent application P.430449.

Hejna, A., Formela, K., Reza Saeb, M., 2015. Processing, mechanical and thermal behavior assessments of polycaprolactone/agricultural wastes biocomposites. Ind. Crop. Prod. 76, 725–733. https://doi.org/10.1016/j.indcrop.2015.07.049

Hejna, A., Haponiuk, J., Piszczyk, Ł., Klein, M., Formela, K., 2017. Performance properties of rigid polyurethane-polyisocyanurate/brewers' spent grain foamed composites as function of isocyanate index. e-Polymers 17 (5), 427–437. https://doi.org/10.1515/epoly-2017-0012

Hejna, A., Sulyman, M., Przybysz, M., Saeb, M.R., Klein, M., Formela, K., 2020. On the correlation of lignocellulosic filler composition with the performance properties of poly(ε-caprolactone) based biocomposites. Waste Biomass Valori. 11, 1467–1479. https://doi.org/10.1007/s12649-018-0485-5

Horvath, Z.H., Halasz-Fekete, M., 2005. Instrumental colour measurement of paprika grist. Ann. Fac. Eng. Hunedoara 3, 101–106.

Hunt, R.W.G., 2004. The Reproduction of Colour (6th ed.). Wiley, Chichester, UK.

International Commission on Illumination, 1978. Recommendations on uniform color spaces, color-difference equations, psychometric color terms. Bureau central de la C.I.E., Paris, France.

Iyer, K.A., Zhang, L., Torkelson, J.M., 2015. Direct use of natural antioxidant-rich agro-wastes as thermal stabilizer for polymer: Processing and recycling. ACS Sustain. Chem. Eng. 4 (3), 881–889. https://doi.org/10.1021/acssuschemeng.5b00945

Kao, S.V., Allison, G.R., 1984. Residence time distribution in a twin screw extruder. Polym. Eng. Sci. 24 (9), 645–651. https://doi.org/10.1002/pen.760240906

Kargarzadeh, H., Huang, J., Lin, N., Ahmad, I., Mariano, M., Dufresne, A., Thomas, S., Gałęski, A., 2018. Recent developments in nanocellulose-based biodegradable polymers, thermoplastic polymers, and porous nanocomposites. Prog. Polym. Sci. 87, 197–227. https://doi.org/10.1016/j.progpolymsci.2018.07.008

Kargarzadeh, H., Mariano, M., Huang, J., Lin, N., Ahmad, I., Dufresne, A., Thomas, S., 2017. Recent developments on nanocellulose reinforced polymer nanocomposites: A review. Polymer 132, 368–393. https://doi.org/10.1016/j.polymer.2017.09.043

Kelly, A.L., Brown, E.C., Coates, P.D., 2006. The effect of screw geometry on melt temperature profile in single screw extrusion. Polym. Eng. Sci. 46 (12), 1706–1714. https://doi.org/10.1002/pen.20657

Kim, J.M., Shin, M., 2014. Effects of particle size distributions of rice flour on the quality of gluten-free rice cupcakes. LWT-Food Sci. Tech. 59 (1), 526–532. https://doi.org/10.1016/j.lwt.2014.04.042

Leonard, W., Zhang, P., Ying, D., Fang, Z., 2019. Application of extrusion technology in plant food processing by-products: An overview. Compr. Rev. Food Sci. F. 19 (1), 218–246. https://doi.org/10.1111/1541-4337.12514

Li, W., Winter, M., Kara, S., Herrmann, C., 2012. Eco-efficiency of manufacturing processes: A grinding case. CIRP Ann. 61 (1), 59–62. https://doi.org/10.1016/j.cirp.2012.03.029

Liu, K., 2009. Effects of particle size distribution, compositional and color properties of ground corn on quality of distillers dried grains with solubles (DDGS). Bioresource Technol. 100 (19), 4433–4440. https://doi.org/10.1016/j.biortech.2009.02.067

López, F., Valiente, J.M., Baldrich, R., Vanrell, M., 2005. Fast Surface Grading Using Color Statistics in the CIE Lab Space, in: Marques, J.S., Pérez de la Blanca, N., Pina, P. (Eds.), Pattern Recognition and Image Analysis. IbPRIA 2005. Springer, Berlin, Heidelberg, pp. 666-673. https://doi.org/10.1007/11492542_81

Lynch, K.M., Steffen, E.J., Arendt, E.K., 2016. Brewers' spent grain: a review with an emphasis on food and health. J. I. Brewing 122 (4), 553–568. https://doi.org/10.1002/jib.363

Mahmood, A.S.N., Brammer, J.G., Hornung, A., Steele, A., Poulston, S., 2013. The intermediate pyrolysis and catalytic steam reforming of Brewers spent grain. J. Anal. Appl. Pyrol. 103, 328–342. https://doi.org/10.1016/j.jaap.2012.09.009

Maillard, L.C., 1912. Action des acides amines sur les sucres; formation de melanoidines par voie méthodique. Compt. Rend. 154, 66-68.

Market Research Store, 2018. Global Wood Plastic Composites (Wpc) Market Report 2018 - Industry Analysis, Size, Share, Trends, Segment and Forecasts to 2025. https://www.marketresearchstore.com/report/global-wood-plastic-composites-wpc-market-report-2018-303554 (accessed 18 April 2019).

Martins, S.I.F., Jongen, W.M., van Boekel, M.A.J., 2000. A review of Maillard reaction in food and implications to kinetic modelling. Trends Food Sci. Tech. 11 (9-10), 364–373. https://doi.org/10.1016/S0924-2244(01)00022-X

Meneses, N.G., Martins, S., Teixeira, J.A., Mussatto, S.I., 2013. Influence of extraction solvents on the recovery of antioxidant phenolic compounds from brewer's spent grains. Sep. Purif. Technol. 108, 152–158. https://doi.org/10.1016/j.seppur.2013.02.015

Mohsin, G.F., Schmitt, F.J., Kanzler, C., Dirk Epping, J., Flemig, S., Hornemann, A., 2018. Structural characterization of melanoidin formed from d -glucose and l -alanine at different temperatures applying FTIR, NMR, EPR, and MALDI-ToF-MS. Food Chem. 245, 761–767. https://doi.org/10.1016/j.foodchem.2017.11.115

Moraczewski, K., Stepczyńska, M., Malinowski, R., Karasiewicz, T., Jagodziński, B., Rytlewski, P., 2019. The Effect of Accelerated Aging on Polylactide Containing Plant Extracts. Polymers 11(4), 575. https://doi.org/10.3390/polym11040575

Morales, F.J., van Boekel, M.A.J.S., 1998. A Study on Advanced Maillard Reaction in Heated Casein/Sugar Solutions: Colour Formation. Int. Dairy J. 8 (10-11), 907–915.

Mussatto, S.I., Dragone, G., Roberto, I.C., 2006. Brewer's spent grain: generation, characteristics and potential applications. J. Cereal Sci. 43, 1-14. https://doi.org/10.1016/j.jcs.2005.06.001

Offiah, V., Kontogiorgos, V., Falade, K.O., 2018. Extrusion processing of raw food materials and by-products: A review. Crit. Rev. Food Sci. 59 (18), 2979–2998. https://doi.org/10.1080/10408398.2018.1480007

Ott, R.L., 1964. Mechanism of the mechanical degradation of cellulose. J. Polym. Sci. Part A 2 (2), 973–982. https://doi.org/10.1002/pol.1964.100020232

Pastoriza, S., Rufián-Henares, J.A., 2014. Contribution of melanoidins to the antioxidant capacity of the Spanish diet. Food Chem. 164, 438–445. https://doi.org/10.1016/j.foodchem.2014.04.118

Rasid, R., Wood, A.K., 2003. Effect of process variables on melt temperature profiles in extrusion process using single screw plastics extruder. Plast. Rubber Compos. 32 (5), 187–192. https://doi.org/10.1179/146580103225002731

Revert, A., Reig, M., Seguí, V.J., Boronat, T., Fombuena, V., Balart, R., 2015. Upgrading brewer's spent grain as functional filler in polypropylene matrix. Polym. Compos. 38 (1), 40–47. https://doi.org/10.1002/pc.23558

Rivero-Pérez, M.D., Pérez-Magariño, S., González-San José, M.L., 2002. Role of melanoidins in sweet wines. Anal. Chim. Acta 458 (1), 169–175. https://doi.org/10.1016/s0003-2670(01)01591-4

Rol, F., Karakashov, B., Nechyporchuk, O., Terrien, M., Meyer, V., Dufresne, A., Belgacem, M.N., Bras, J., 2017. Pilot-Scale Twin Screw Extrusion and Chemical Pretreatment as an Energy-Efficient Method for the Production of Nanofibrillated Cellulose at High Solid Content. ACS Sustain. Chem. Eng. 5 (8), 6524–6531. https://doi.org/10.1021/acssuschemeng.7b00630

Rufián-Henares, J.A., Morales, F.J., 2007. Functional properties of melanoidins: In vitro antioxidant, antimicrobial and antihypertensive activities. Food Res. Int. 40 (8), 995–1002. https://doi.org/10.1016/j.foodres.2007.05.002

Sahputra, I.H., Alexiadis, A., Adams, M.J., 2019. Effects of moisture on the mechanical properties of microcrystalline cellulose and the mobility of the water molecules as studied by the hybrid molecular mechanics-molecular dynamics simulation method. J. Polym. Sci. Pol. Phys. 57 (8), 454–464. https://doi.org/10.1002/polb.24801

Sarasini, F., Tirillò, J., Zuorro, A., Maffei, G., Lavecchia, R., Puglia, D., Dominici, F., Luzi, F., Valente, T., Torre, L., 2018. Recycling coffee silverskin in sustainable composites based on a poly(butylene adipate-co-terephthalate)/poly(3-hydroxybutyrate-co-3-hydroxyvalerate) matrix. Ind. Crop. Prod. 118, 311–320. https://doi.org/10.1016/j.indcrop.2018.03.070

Silva, G.G.D., Guilbert, S., Rouau, X., 2011. Successive centrifugal grinding and sieving of wheat straw. Powder Technol. 208 (2), 266–270. https://doi.org/10.1016/j.powtec.2010.08.015

Sun, C., Liu, R., Ni, K., Wu, T., Luo, X., Liang, B., Zhang, M., 2016. Reduction of particle size based on superfine grinding: Effects on structure, rheological and gelling properties of whey protein concentrate. J. Food Eng. 186, 69–76. https://doi.org/10.1016/j.jfoodeng.2016.03.002

Suparno, M., Dolan, K.D., Ng, P.K.W., Steffe, J.F., 2010. Average shear rate in a twin-screw extruder as a function of degree of fill, flow behavior index, screw speed and screw configuration. J. Food Process Eng. 34 (4), 961–982. https://doi.org/10.1111/j.1745-4530.2009.00381.x

The Brewers of Europe, 2018. Beer statistics, 2018 edition. https://brewersofeurope.org/uploads/mycms-files/documents/publications/2018/EU-beer-statistics-2018-web.pdf (accessed 18 April 2019).

Wang, H.Y., Qian, H., Yao, W.R., 2011. Melanoidins produced by the Maillard reaction: Structure and biological activity. Food Chem. 128 (3), 573–584. https://doi.org/10.1016/j.foodchem.2011.03.075

Vanreppelen, K., Vanderheyden, S., Kuppens, T., Schreurs, S., Yperman, J., Carleer, R., 2014. Activated carbon from pyrolysis of brewer's spent grain: Production and adsorption properties. Waste Manage. Res. 32 (7), 634–645. https://doi.org/10.1177/0734242X14538306

Waters, D.M., Jacob, F., Titze, J., Arendt, E.K., Zannini, E., 2012. Fibre, protein and mineral fortification of wheat bread through milled and fermented brewer's spent grain enrichment. Eur. Food Res. Technol. 235 (5), 767–778. https://doi.org/10.1007/s00217-012-1805-9

Villamiel, M., del Castillo, M.D., Corzo, N., 2006. 4. Browning Reactions, in: Hui, Y.H., Nip, W.K., Nollet, L.M.L., Paliyath, G., Simpson, B.K. (Eds.), Food biochemistry and food processing. Wiley-Blackwell, New York, pp. 71–100. https://doi.org/10.1002/9781118308035.ch4

Wu, H.B., Yun, J.M., Li, Y., Han, P., 2011. Relationship between malt chroma and melanoidin at different drying conditions. Journal of Gansu Agricultural University 45, 130–133.

Yeh, A.I., Hwang, S.J., Guo, J.J., 1992. Effects of screw speed and feed rate on residence time distribution and axial mixing of wheat flour in a twin-screw extruder. J. Food Eng. 17 (1), 1–13. https://doi.org/10.1016/0260-8774(92)90061-A

Yilmaz, Y., Toledo, R., 2005. Antioxidant activity of water-soluble Maillard reaction products. Food Chem. 93 (2), 273–278. https://doi.org/10.1016/j.foodchem.2004.09.043

Zajchowski, S., Ryszkowska, J., 2009. Kompozyty polimerowo-drzewne – charakterystyka ogólna oraz ich otrzymywanie z materiałów odpadowych. Polimery 54 (10), 674-682.

Zedler, Ł., Colom, X., Cañavate, J., Saeb, M.R., Haponiuk, J.T., Formela, K., 2020. Investigating the impact of curing system on structure-property relationship of natural rubber modified with brewery by-product and ground tire rubber. Polymers 12, 545. https://doi.org/10.3390/polym12030545

Zedler, Ł., Colom, X., Saeb, M.R., Formela, K., 2018. Preparation and characterization of natural rubber composites highly filled with brewers' spent grain/ground tire rubber hybrid reinforcement. Compos. Part B-Eng. 145, 182–188. https://doi.org/10.1016/j.compositesb.2018.03.024

- Upcycling of brewers' spent grain (BSG) by treatment of twin-screw extruder
- Evaluation of temperature, throughput and rotational speed on properties of BSG
- Adjustment of extrusion parameters leads to desired appearance and properties of BSG
- Treated BSG was characterized by higher thermal stability and antioxidant activity
- Extrusion of BSG allows extend its applications in wood polymer composites technology